Supporting Information

Lucas et al. 10.1073/pnas.1210807110

SI Materials and Methods

Plasmid Constructions. The H2B-RFP fusion driven by the Ubiquitin promoter (pUBI10::H2B–RFP) was obtained by Gateway-mediated cloning of Histone 2B (H2B) (AT5G22880) under the control of the UBI promoter (1).

Statistical Shape Analysis. ***Procruste analysis.*** Suppose we are considering a set of 2D discrete configurations of points, each of which consists of k landmarks. We represent the coordinates of the landmarks of the i-th configuration as a $k \times 2$ matrix whose first column gives the *x*-coordinates and whose second column gives the *y*-coordinates. The centroid of such a configuration is calculated by taking the mean of the *x*-coordinates and the mean of the *y*-coordinates. The centroid size is the square root of the sum of squares of the Euclidean distances of the k landmarks from the centroid.

To standardize the set of configurations, for each configuration independently we subtract the centroid from each of the k landmarks and divide the coordinates by the centroid size. This gives us centered configurations whose centroid size is 1. These objects may therefore be thought of as points on the k-dimensional sphere and are known as preshapes, as rotation is yet to be removed. All possible rotations of the centered, scaled configurations have the same geometric arrangement, so we define the shape of a configuration as the set of all possible rotations of the preshape.

It can be shown that it is possible to think of the shapes of all possible configurations with k landmarks in two dimensions as points on a mathematical surface (technically a manifold). Further, it is possible to define a metric on the manifold, thereby making it a Riemannian manifold. Given two configurations, the Procrustes distance between them is simply the great circle distance on the k-dimensional sphere between the first configuration and the second configuration after optimally rotating the second configuration such that the sum of squares of Euclidean distances between the landmarks of the two configurations is minimized. The Procrustes metric is a monotone increasing function of the minimum sum of squares obtained on rotation of one of the preshapes relative to the other.

Generalized Procrustes Analysis involves the optimal registration of a set of shapes to minimize an overall sum of square errors. For more than two shapes this requires an iterative procedure, and the details are given in chapter 5 of Dryden and Mardia (2).

Shape comparison. Shape space is non-Euclidean. However, it is possible to construct a Euclidean tangent space to shape space at a particular point for the purposes of visualization. Shapes are projected into the tangent space and the axes of the tangent space are the principal components of the tangent space coordinates. For details, see pp. 71–76 of Dryden and Mardia (2). Provided the objects in the dataset are quite close in shape, which is the case for all of the lateral root primordia (LRP) examples considered, using the Euclidean distance in the tangent space is a good approximation to the shape distances in the shape space.

In Fig. S8*A*, the mean shapes of the LRPs for stages 1–6 of the WT and the aurora mutant along with stages 1–5 of the J0631–axr3–glucocorticoid receptor are shown superimposed for each of the plant types separately. The shapes have each been rotated such that the line between the two ends of the base of each shape is vertical and the bulge of the LRP is to the right. In Fig. S8*B*, the mean shapes have been projected into tangent space. In this case the first two principal components explain just over 90% of the variability in the dataset. The point (0,0) corresponds to the mean shape of the 17 shapes in the figure.

Fig. S8*B* clearly shows that the shapes of the LRPs in the Dexamethasome-induced J0631–axr3–GR construct do not develop in the same way as in WT or in the aurora mutant. No LRPs were observed in stage 6 or later, and the mean shapes for stages 1–5 are densely bunched toward the left of the figure.

1. Grefen C, Donald N, Schumacher K, Blatt MR (2010) A ubiquitin-10 promoter-based vector set for fluorescent protein tagging facilitates temporal stability and native protein distribution in transient and stable expression studies. *Plant J* 64(2):355–365.

2. Dryden IL, Mardia KV (1998) *Statistical Shape Analysis* (Wiley, New York).

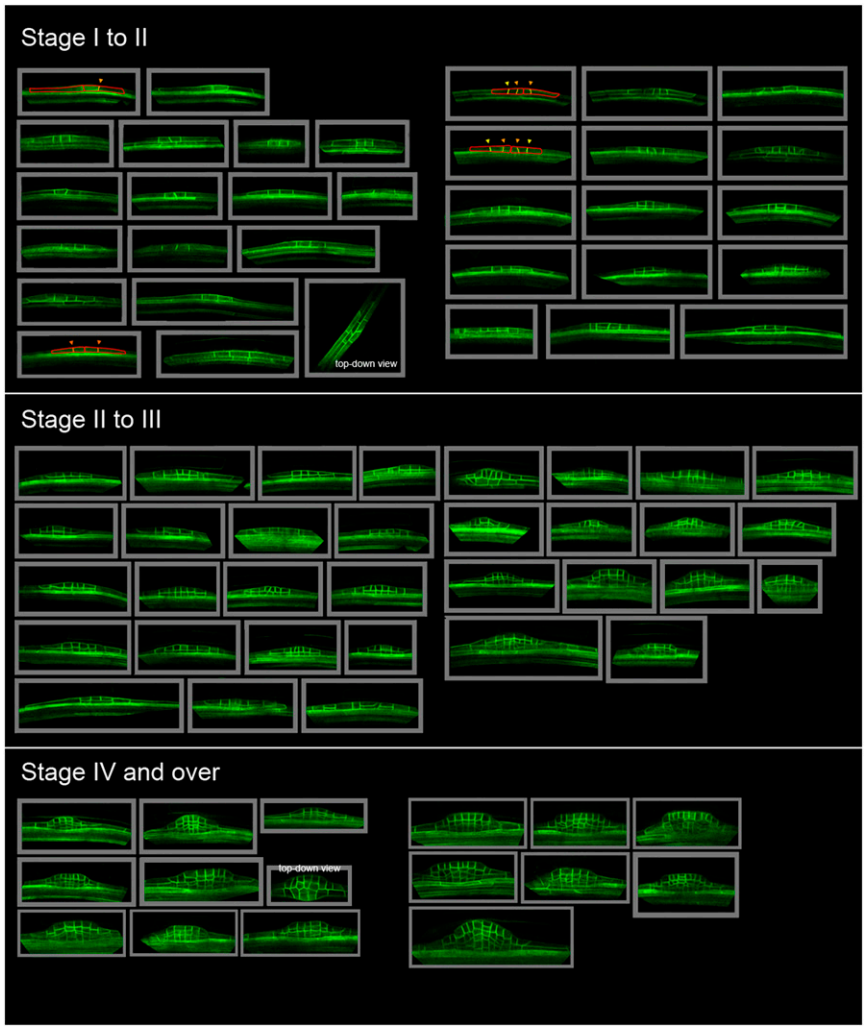

Fig. S1. LRP tissular pattern diversity. Collection of confocal images of primordia that express *AUX1–YFP* = AUX1-YFP fusion driven by the native AUX1 promoter (pAUX1:AUX1–YFP), illustrating the variability of tissular pattern between individual LRPs. Primordia were imaged as stacks of 100–150 images at 0.5 μm z-spacing with a Plan Fluor 20.0×/0.50 or 40.0×/0.75 lenses.

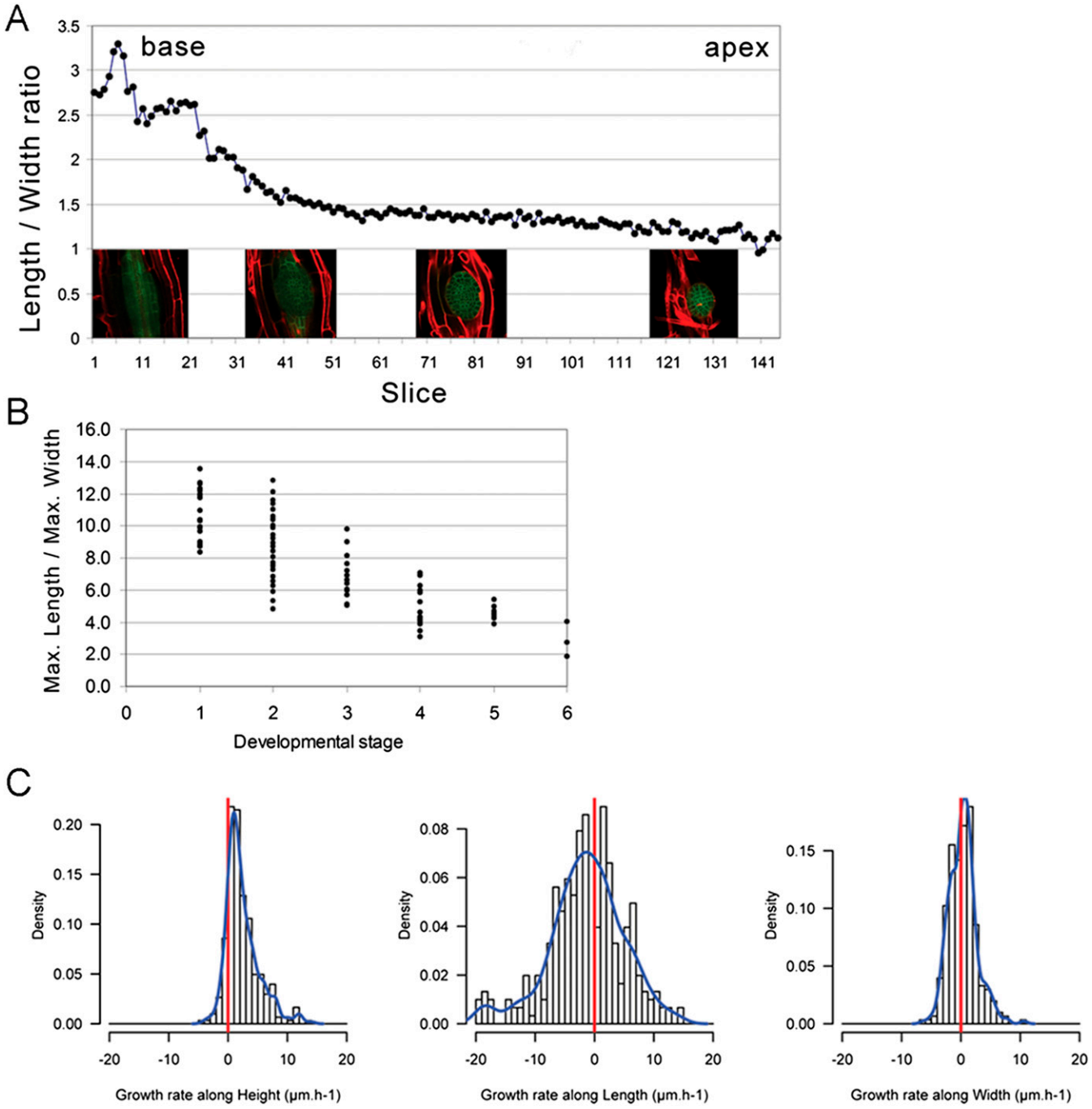

Fig. S2. Local and global ellipsoidal character of lateral root primordial. (*A*) Local ellipsoidal character of an emerging LRP. Ellipsoidal character was measured for each optical slice ($n = 150$) of a front-view confocal z-stack, from base (along the vascular strands of the main root) to apex. Insets illustrate the shape of the LRP for different optical slices. (*B*) Local ellipsoidal character for LRPs at different developmental stages. The z-stacks were used to rebuild simple volumetric reconstruction of LRP. Maximum length and width of the LRPs were measured from a top-down view of the volumetric reconstruction, encompassing the whole LRP. (*C*) Histograms of the distributions of the hourly growth rates for three individual lateral root primordium along the height, length, and width axis.

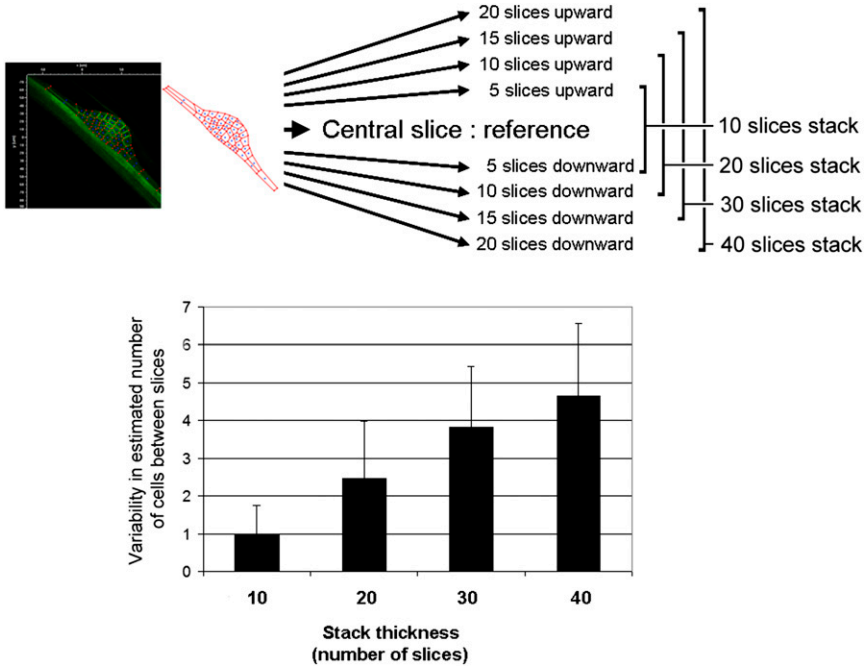

Fig. S3. Transversal variability of primordia cellular structures. Number of cells was measured for median optical slice of lateral root primordial, as well as 5, 10, 15, and 20 slices up and down of this median slice (with a mean distance between slices of 0.5 microns). The variability in terms of estimated number of cells between slices depending on the distance from the median optical slice was determined from stage VI, V, and VI primordia (n = 30).

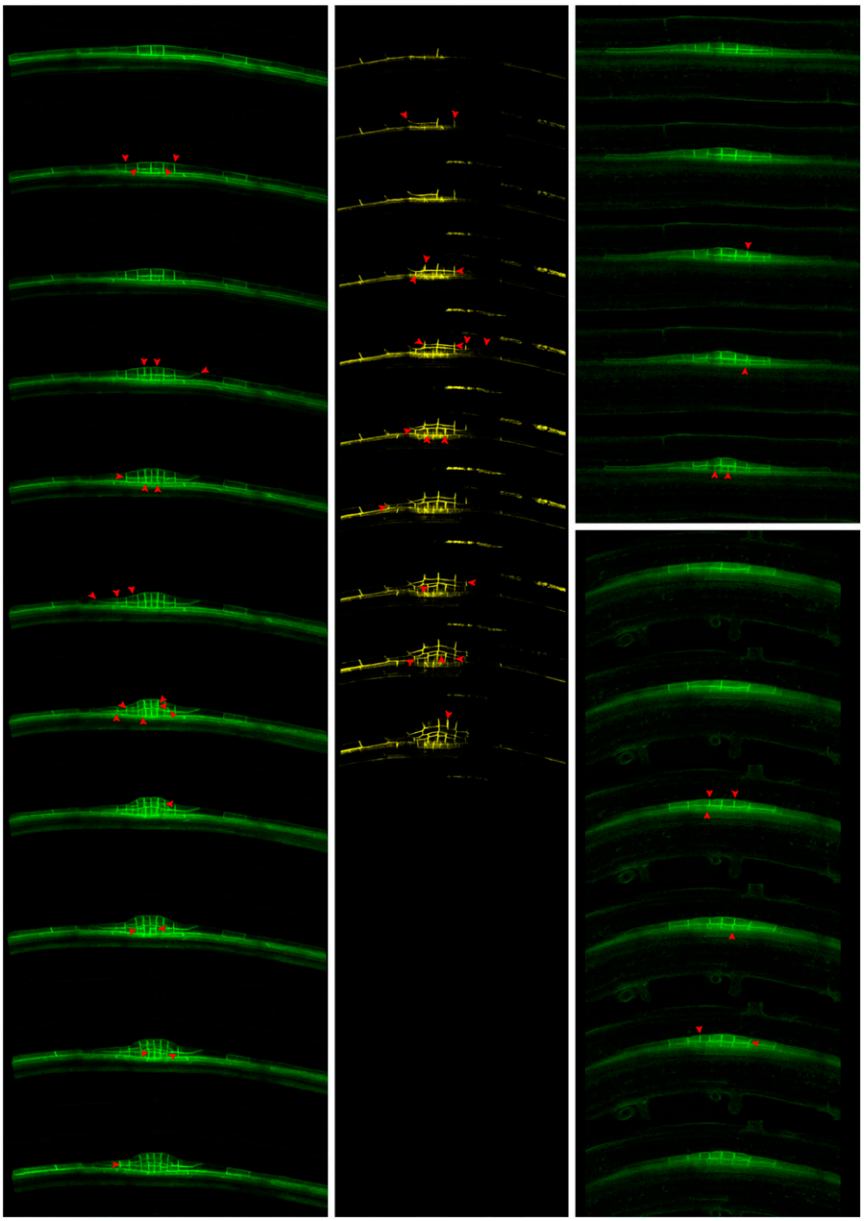

Fig. S4. LRP cell division sequence diversity. Sequences of cell divisions (red arrows) observed in time-lapse confocal microscopy using pAUX1:AUX1–YFP (green) or plasmamembrane-YFP reporter driven by the Ubiquitin promoter (WAVE131–YFP) (yellow) markers. Time between successive acquisitions is 2 h. Primordia were imaged as stacks of 150 images at 0.5 μm z-spacing with a Plan Fluor 20.0×/0.50 lens.

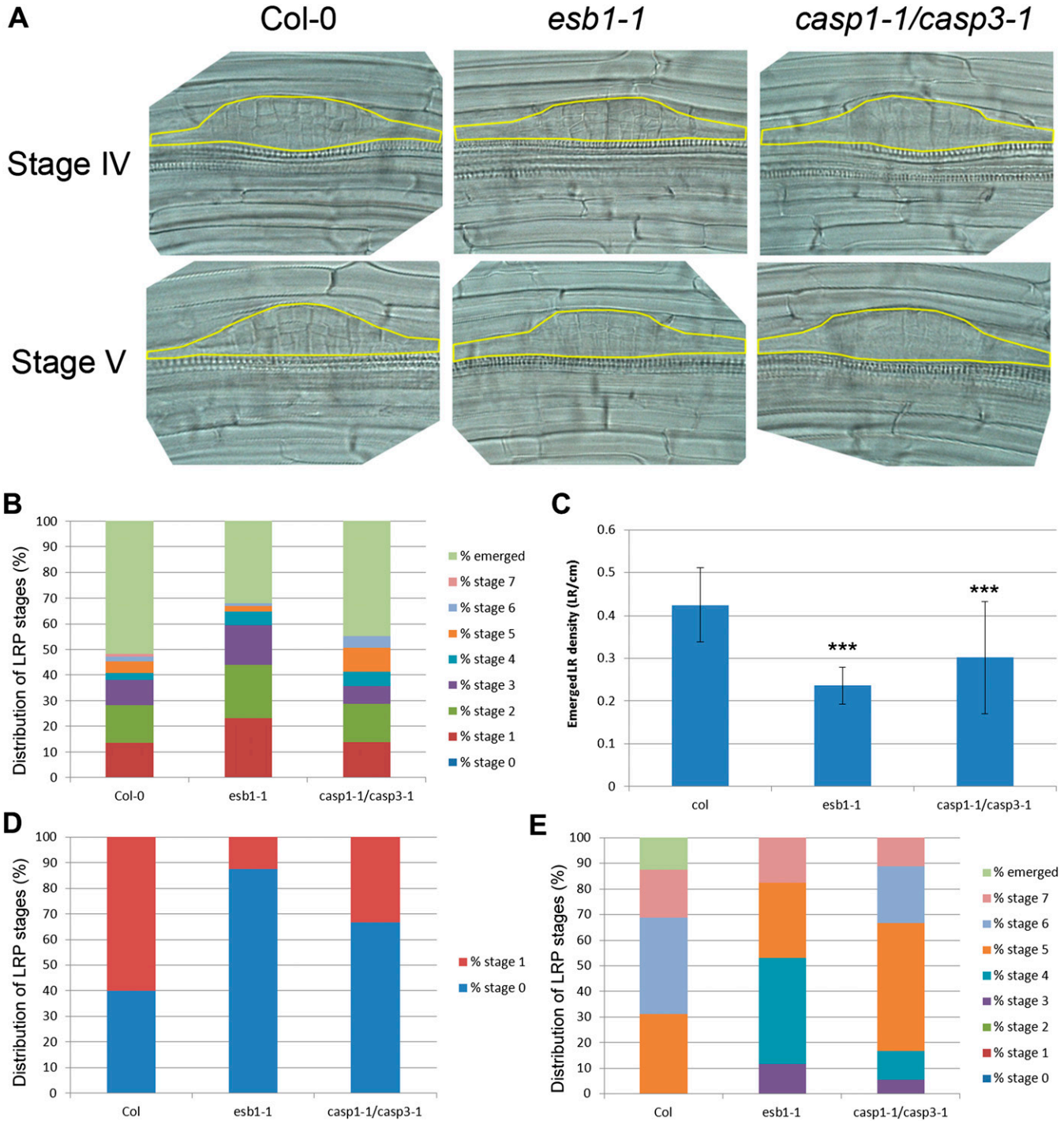

Fig. S5. LRP development in enhanced suberin1 (*esb1-1*) and *casparian strip membrane domain protein* (*casp1-1*)/*casp3-1* lines. (*A*) Impact of *esb1-1* single mutation or *casp1-1/casp3-1* double mutation on primordia shape development. LRP shapes are outlined in yellow. (*B*) Staging of LRP in *esb1-1* or *casp1-1/casp3-1* 10 d after germination. (*C*) Emerged lateral root density in *esb1-1* or *casp1-1/casp3-1* 10 d after germination. Statistical analysis showed that lateral root density is significantly reduced in *esb1-1* ($P < 0.001$) and *casp1-1/casp3-1* ($P < 0.05$). (*D*) Staging of LRP in *esb1-1* or *casp1-1/casp3-1* 18 h after gravistimulation. (*E*) Staging of LRP in *esb1-1* or *casp1-1/casp3-1* 42 h after gravistimulation.

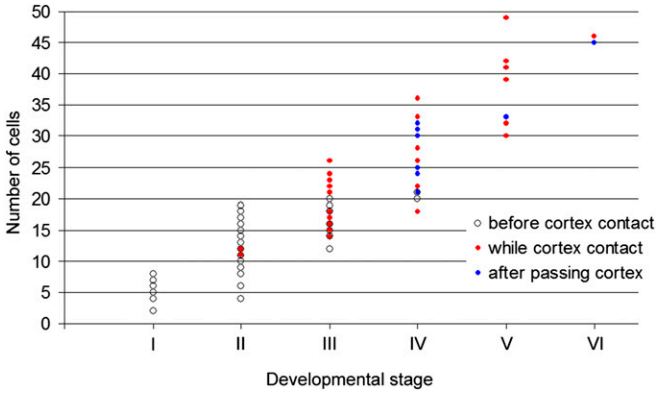

Fig. S6. Cell divisions continue while the primordium is blocked against the endodermis–cortex junction. Contact between primordia and cortex layer was determined in confocal microscopy using pAUX1:AUX1–YFP or WAVE131–YFP markers. The plot indicates the number of cells in visible lateral root primordia median slices (n = 117).

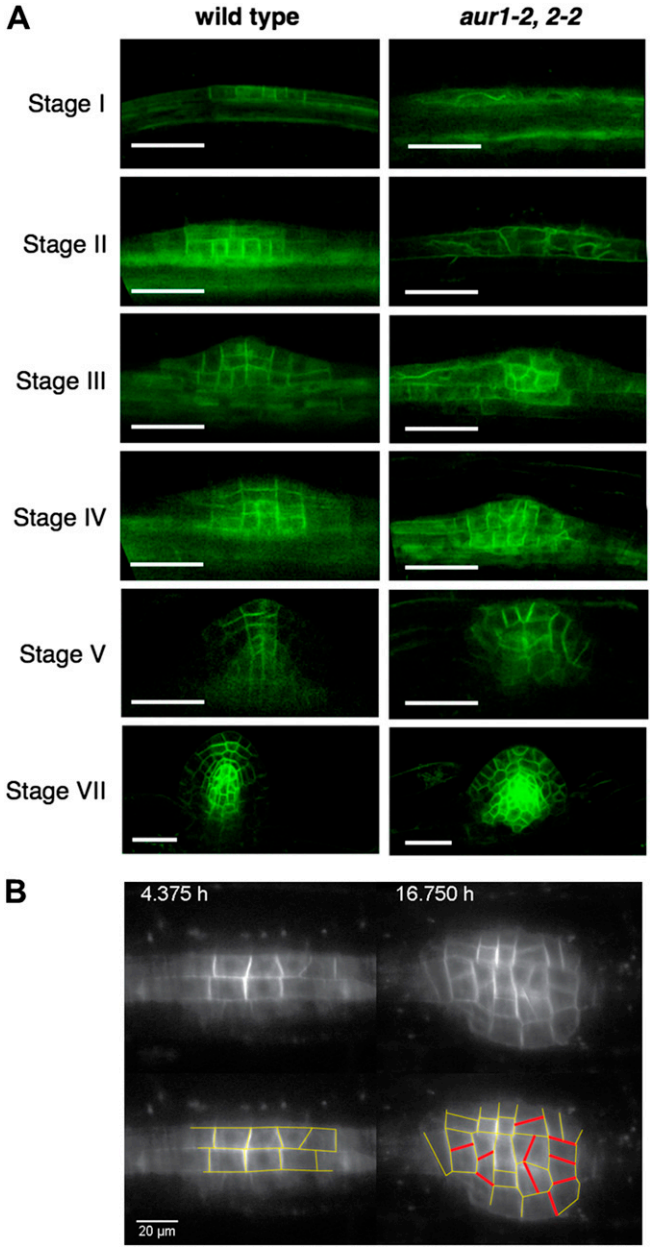

Fig. S7. Altered division planes in *aur1-2;2-2* double mutant. (*A*) Confocal sections of a wild-type or *aur1-2;2-2* mutant expressing PIN1-YFP fusion driven by the native PIN1 promoter in the *aurora* double mutant background (pPIN1:PIN1–GFP) (scale bar, 50 μm). (*B*) (*Upper* row) Frontal view of light-sheet imaging of a *aur1-2;2-2* mutant lateral root primordium that stably expresses pPIN1:PIN1–GFP. (*Lower* row) Schematic representation of the constitution of circular buttresses by the tangential and radial cell divisions (in red). A stack of images were collected every 7.5 min with a pair of Carl Zeiss *N*-Achroplan 40×/0.75 W (detection) and Carl Zeiss EC Plan-Neofluar 5×/0.16 (illumination) lenses.

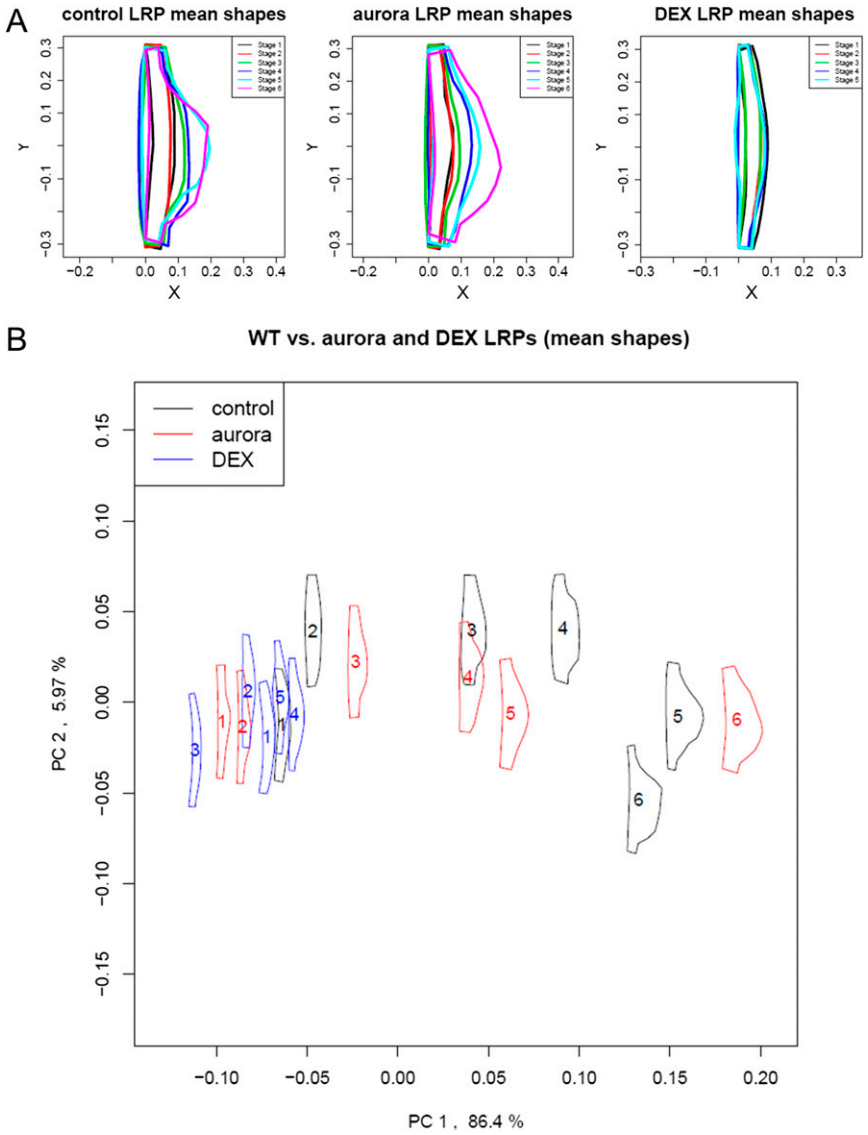

Fig. S8. Statistical shape analysis of DEX-treated J0631>>axr3-1 fusion to the glucocorticoid receptor controlled by the GAL4 regulated Upstream Activation Sequence (UASaxr3GR), *aur1-2;2-2*, and wild-type LRP development. (*A*) LRP mean shapes for stages I to VI in wild-type, *aur1-2;2-2* double mutant, and DEX-treated J0631>>UASaxr3GR. (*B*) Distribution of wild-type, *aur1-2;2-2* double mutant, and DEX-treated J0631>>UASaxr3GR LRP shapes in 2D shape space.

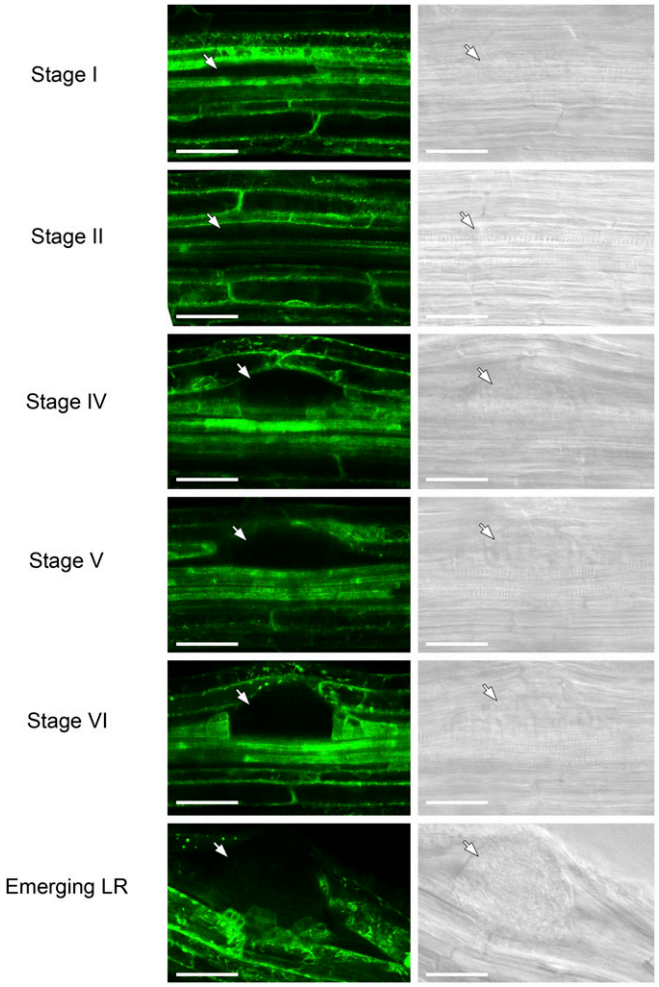

Fig. S9. LRPs are not targeted for transactivation in the J0631 transactivation line. J0631 plants were vertically grown for 1 wk before confocal imaging of LRP. Comparison between confocal images of GFP (green) marker expressed in tissues targeted for transactivation in the J0631 line (*Left* column) and corresponding bright field view (*Right* column) revealed that LRPs (white arrow) are not targeted for transactivation in the J0631 line until late after emergence (scale bar, 50 μm).

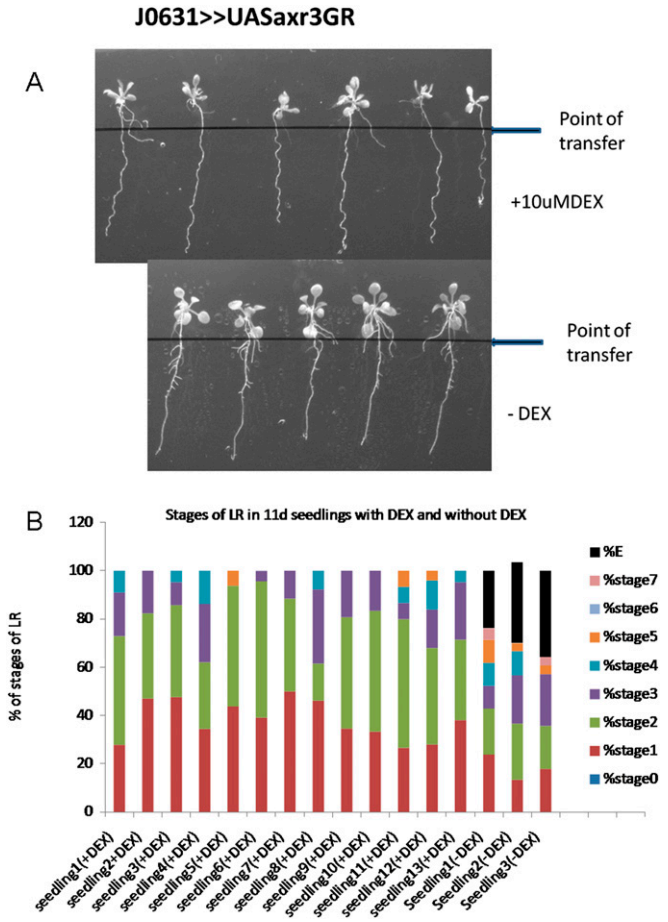

Fig. S10. LRP development in J0631>>UASaxr3GR line. (*A*) Whole seedling imaging in J0631>>UASaxr3GR plants 5 d after transfer on 10 μM DEX or non-DEX media. (*B*) Staging of LRP in J0631>>UASaxr3GR plants 5 d after transfer on 10 μM DEX or non-DEX media.

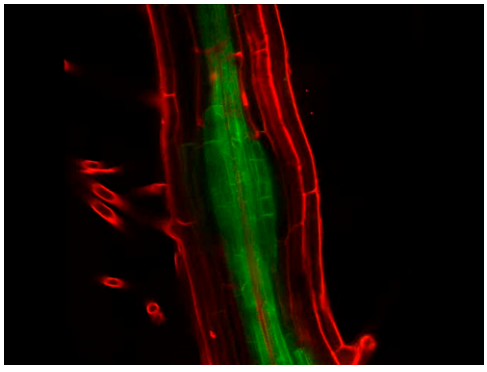

Movie S1. Front view of an emerging lateral root primordium. Confocal z-stack at 0.5 μm z-spacing of marked lateral root primordium expressing pAUX1: AUX1–YFP and counterstained with propidium iodide. Primordium was imaged as a stack of 200 images at 0.5 μm z-spacing with a Plan Fluor 40.0×/0.75 lens.

Movie S1

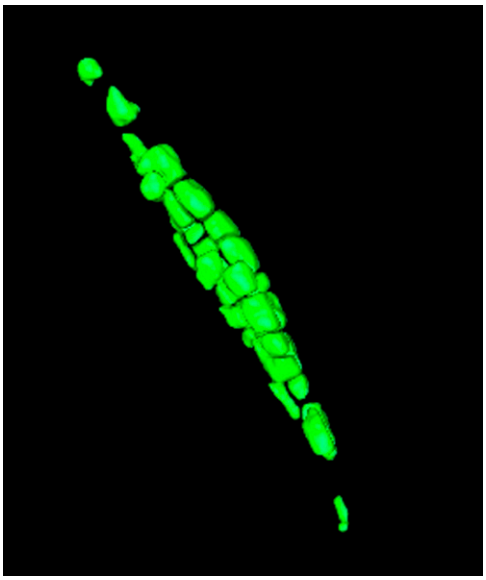

Movie S2. Three-dimensional reconstruction of a stage II lateral root primordium. Confocal z-stack at 0.5 μm z-spacing of marked lateral root primordium expressing pAUX1:AUX1–YFP and counterstained with propidium iodide was treated according to the reconstruction protocol described by ref. 1 to generate 3D reconstruction. Primordium was imaged as a stack of 50 images at 0.5 μm z-spacing with a Plan Fluor 40.0×/0.75 lens.

Movie S2

1. Fernandez R, et al. (2010) Imaging plant growth in 4D: Robust tissue reconstruction and lineaging at cell resolution. *Nat Methods* 7(7):547–553.

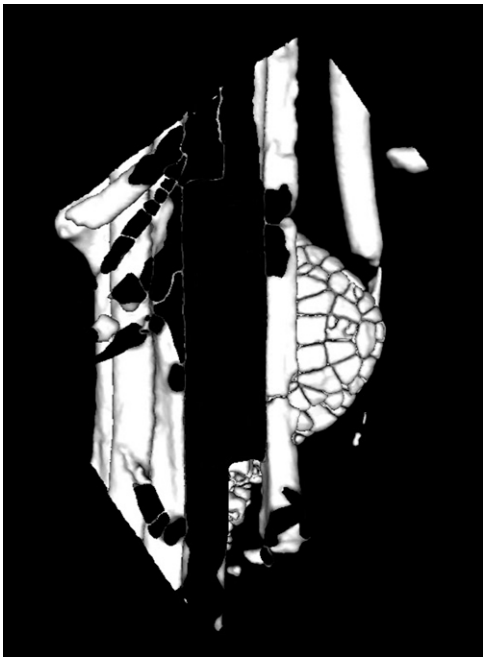

Movie S3. Three-dimensional reconstruction of an emerging lateral root primordium. Confocal z-stack at 0.5 μm z-spacing of marked lateral root primordium expressing pAUX1:AUX1–YFP and counterstained with propidium iodide was treated according to the reconstruction protocol described by ref. 1 to generate 3D reconstruction. Primordium was imaged as a stack of 100 images at 0.5 μm z-spacing with a Plan Fluor 40.0×/0.75 lens.

Movie S3

1. Fernandez R, et al. (2010) Imaging plant growth in 4D: Robust tissue reconstruction and lineaging at cell resolution. *Nat Methods* 7(7):547–553.

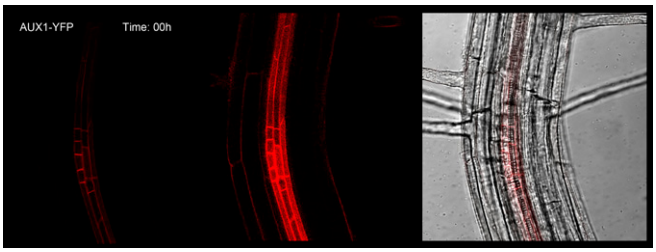

Movie S4. Build-up of structural pressure in a developing lateral root primordium. Confocal observation of a LRP induced by gravistimulation in the pAUX1:AUX1–YFP transgene line. The sudden LRP shape change between 16 and 18 h after gravistimulation suggests that structural pressure is building up within the LRP before that event. (*Left*) LRP cellular structure is marked by membrane-bound AUX1–YFP (red). (*Middle*) Same images at a higher saturation level, highlighting the outer tissues (due to low-level pAUX1:AUX1–YFP expression). (*Right*) Superimposition of brightfield and confocal images. Primordium was imaged every 2 h as a stack of 300 images at 0.5 μm z-spacing with a Plan Fluor 40.0×/0.75 lens.

Movie S4

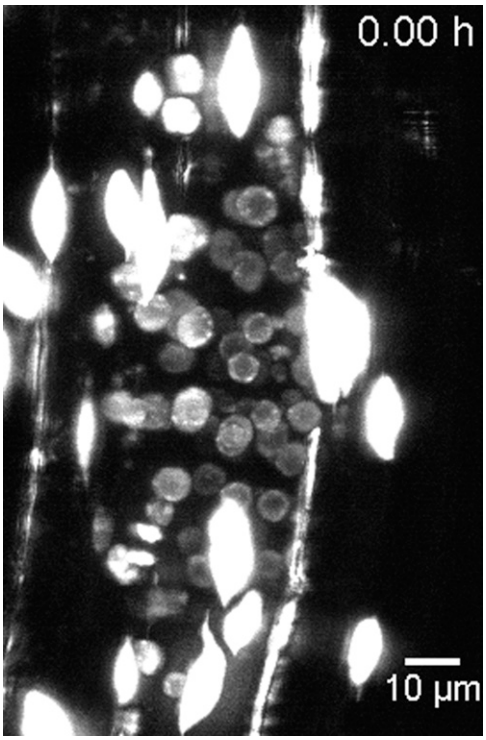

Movie S5. The LRP ruptures the endodermis within minutes. Light-sheet microscopy time-lapse imaging of a lateral root primordium that stably expresses H2B-RFP fusion driven by the Ubiquitin promoter (pUB10:H2B–RFP). A stack of images were collected every 7.5 min for 9 h with a pair of Carl Zeiss *N*-Achroplan 40×/0.75 W (detection) and Carl Zeiss EC Plan-Neofluar 5×/0.16 (illumination) lenses (scale bar, 10 μm).

Movie S5

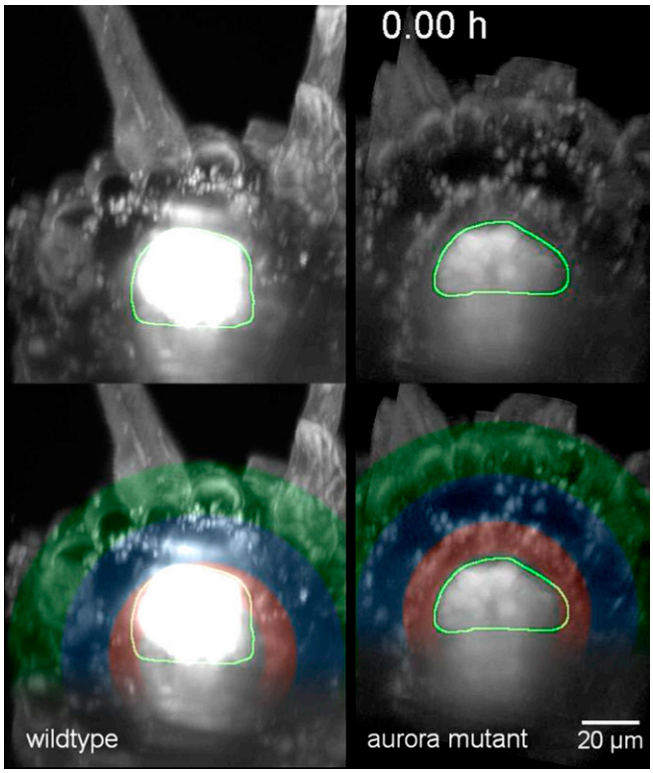

Movie S6. LRP growth in wild-type and *aur1-2;2-2* double mutant (bottom view). (*Upper* row) Light-sheet microscopy time-lapse imaging of a lateral root primordium that stably expresses pPIN1:PIN1–GFP in wild-type (*Left*) and in *aur1-2;2-2* mutant (*Right*) background. (*Lower* row) Schematic highlight of the three overlaying cell layers (red, endodermis; blue, cortex; green, epidermis). A stack of images were collected every 7.5 min for 29 h with a pair of Carl Zeiss *N*-Achroplan 40×/0.75 W (detection) and Carl Zeiss EC Plan-Neofluar 5×/0.16 (illumination) lenses. Each stack contains 388 planes spaced 0.645 μm along the *z*-axis (scale bar, 20 μm).

Movie S6